The Drosophila ovary produces two waves of adult follicles and a novel pupal wave that turns over

Wayne Yunpeng Fu[1,2,3] and Allan C Spradling[1,2,3,4]

[1]Carnegie Institution for Science

[2]Howard Hughes Medical Institute

[3]Department of Biology, Johns Hopkins University

3520 San Martin Dr.

Baltimore, MD 21218

[4]correspondence: spradling@carnegiescience.edu

ABSTRACT

Ovarian follicles in Drosophila and many other species are thought to develop using a single pathway. In contrast, we show by lineage tracing ~3,000 single-cell clones that three follicle "waves" arise in pupae, each following a distinct developmental program. 40 of the ~100 larval primordial germ cells (PGCs) associate with niches to become germline stem cells (GSCs) that produce wave 2 follicles throughout adulthood. Wave 1.5 follicles develop directly from most of the remaining PGCs to become the first ~100 follicles present at eclosion, more than previously expected. Wave 1.5 follicles acquire their follicular coverage from two follicle stem cells (FSCs) that are specifically replaced by new FSCs for wave 2. A novel wave 1 population amplifies rapidly to reach 250-350 germ cells, but soon undergoes programmed degeneration and exits the ovary along with somatic cells as they release lipid-enriched vacuoles. A subpopulation of testis germ cells behave in a similar manner. We propose that wave 1 germ cell breakdown contributes to the concomitant but unexplained pharate adult ecdysone pulse that mediates adult tissue development.

Keywords

germ cell, ovarian follicle wave, germline stem cell, follicle stem cell, Drosophila melanogaster , pupal ovary

INTRODUCTION

Some species generate subclasses of ovarian follicles, in spatially or temporally separated groups known as waves (DeFalco and Capel, 2009; Eppig and Handel, 2012; Pazdernik and Schedl, 2013). Mammals such as mice generate wave 1 ovarian follicles that grow immediately at birth in the central medullar region, while 95% of follicles, the wave 2, reside in the cortex region and become quiescent as the ovarian reserve (Mork et al., 2012; Rotgers et al., 2018). A recently described third wave of primordial follicles, termed "wave 1.5," develops at the medulla/cortex boundary, arrests for ~ 2 weeks, and produces most the first ovulated oocytes rather than wave 1 (Meinsohn et al., 2021; Yin and Spradling, 2025). Wave 1 follicles generate few if any mature oocytes. They undergo a process classically termed "atresia" (Byskov, 1974), in which most oocytes and granulosa cells turn over, while thecal cells proliferate and interstitial gland cells are recruited. These hormone-producing cells reorganize into a gland-like region that synthesizes mainly androgenic steroids during a sensitive period of embryonic development (Trova et al., 2021). Drosophila ovaries may contain similar follicle waves, whose identification requires studying in detail how the ovary develops under control of the steroid hormone ecdysone during larval and pupal stages (Figure 1A; King et al., 1968, King, 1970; Sahut-Barnola et al., 1995; Godt and Laski, 1995; Forbes et al., 1996; Couderc et al., 2002; Camara et al., 2019).

In Drosophila, ovarian follicles develop in ordered strings known as ovarioles that begin with a germarium region containing stem cells producing both germline and somatic cells (Figure 1B). 2-3 GSCs reside in a niche consisting of terminal filament (TF) and cap cells (CC) at the germarium tip where they give rise to daughter cells called cystoblasts (CB) that undergo 4 rounds of cyst division to form 16-cell germline cysts consisting of one ooycte and 15 nurse cells (Figure 1C, 1E). Two follicle stem cells (FSCs) reside midway through the germarium on opposite sides at the junction

between regions 2a and 2b where cysts switch from a temporary covering of squamous escort cells (ECs) to a monolayer of epithelial follicle cells (Margolis and Spradling, 1995). Both FSCs are maintained in niches at the 2a/2b junction by local escort cells and intercellular signals (Nystul and Spradling, 2007; Sahai-Hernandez and Nystul, 2013).

The embryonic ovary acquires primordial germ cells (PGCs) which proliferate throughout larval development in association with somatic intermingled cells (Wieschaus and Szabad, 1979; Zhu and Xie, 2003; Li et al., 2003; Gilboa and Lehmann, 2006; Ganz et al., 2011; Banish et al., 2021; Rosales-Nieves et al., 2025). A pulse of the steroid hormone ecdysone induces the formation of TFs in third instar larval ovaries that guide ovariole development (Godt and Laski, 1995; Sahut-Barnola et al, 1996; Forbes et al., 1996). Before TFs are completed, a large population of somatic swarm cells migrate from the anterior to the posterior region of the ovary (Couderc et al., 2002). Another key event is GSC niche formation (Lin and Spradling, 1993; Xie and Spradling, 2000; Zhu and Xie, 2003; Song et al., 2002; Song et al., 2007; Gilboa and Lehmann, 2006; Panchal et al., 2017). The TF constitutes the distal part of the GSC niche, whose Notch-dependent development continues during early pupal stages by adding CCs and specialized basement membranes (Zhu and Xie, 2003; Song et al., 2002; Song et al., 2007; Panchal et al., 2017; Yatsenko and Shcherbata, 2018; Diaz-Torres et al., 2021). 30-40 PGCs per ovary enter stem cell niches and become GSCs, but the schedule of GSC activation remains uncertain. About 60 other PGCs were observed to directly undergo oogenesis to generate the first ovulated eggs (Zhu and Xie, 2003; Asaoka and Lin, 2004), but their development has not been fully characterized.

Here we use lineage tracing and developmental studies to identify and characterize three Drosophila follicular waves, which we named based on the three waves of mouse follicles. Directly developing PGCs give rise to "wave 1.5" follicles that produce the first ~100 eggs, after which

follicles are exclusively derived from GSC divisions and are covered with follicle cells derived from distinct FSCs to make up "wave 2" follicles. Unexpectedly, a previously undescribed wave of follicles we term "wave 1" develops even earlier but turns over between 22h and 26h after puparium formation (APF) via an atresia-like process. Wave 1 germ cells break open and release lipophilic cytoplasmic material, before they exit the ovary posterior along with somatic cells. Similar germ cell turnover in the pupal testis takes place at this time, but both ovaries and testes appear fully repaired within a few hours. Wave 1 amplification and extrusion temporally overlaps with the large pharate adult ecdysone pulse (Figure 1A), the source of which has been a longstanding mystery (Dai and Gilbert, 1991; Scanlan et al., 2023). The prothoracic gland produces larval ecdysone pulses but turns over during early pupal stage; an alternative source for the pupal pulses remains to be found. We propose that wave 1 atretic gametes contribute in an unknown manner to the pharate adult ecdysone pulse.

RESULTS

Analyzing ovarian follicle waves by lineage tracing

To obtain a clear picture of follicle waves, we used a background-free lineage labeling system based on heat shock-induced FLP-mediated recombination between chromosome 2L homologs (Harrison and Perrimon, 1994; Margolis and Spradling, 1995; Figure S1A). Heat shock can activate recombination in one daughter of any actively cycling cell, but only a small fraction actually recombines, allowing for single-cell resolution. Moreover, recombination causes only one of the two daughter cells at the next mitosis to become heritably marked (Figure 1D), a property that enables detailed analysis of germline development due to its well-characterized GSC and germline cyst division patterns (Figure 1E, F).

Clone induction was accurately timed ($\pm$2h) by using the short transition period of pupariation as benchmark (see Methods). We induced clones at 4-hour intervals between -2h and 14h (all times refer to APF) and analyzed them either 24 hours later or shortly after eclosion (Figure 1A). All ovarioles were analyzed for somatic cell clones in both germaria and follicles, whereas we found it sufficient to analyze germ cells in only one replicate of each group due to low variability. Altogether, we fully characterized 2,368 germ cell clones and 569 somatic cell clones from 2,270 individual ovarioles (Table S1-S3).

Characterization of wave 2 follicles

We define “wave 2” follicles as those derived from GSCs, and “wave 1.5” as those produced from directly differentiating PGCs. First, we analyzed the GSCs that support wave 2 follicle production throughout adult stage. GSC clones can be recognized in newly eclosed adult ovaries by a marked GSC at the tip of the germarium followed by adjacent marked progeny cysts resulting from GSC asymmetric divisions (Figure 1C, 2A). The number of GSC clones with these properties

increased at 10h to reach a labeling frequency similar to that of the adult GSCs (Figure 2C, blue line). Since lineage marker recombination only requires an active, post-G1 cell cycle state, the labeling rate of a cell population positively correlates with cell number, but not cell cycle length. Therefore, the increased labeling rate at 10h indicates a larger GSC population. Marked GSCs produce an average of 4 marked progeny cysts by eclosion, and since their first division product is unmarked (Figure 1F), pupal GSCs usually undergo 5 divisions during pupal development (Figure 2C, orange line). GSC division number stayed constant across the five labeling time points, indicating no GSC division until at least 10h. Around 4% of ovarioles with GSC clones had all GSCs labeled (Figure 2D-D'). They demonstrate that wave 2 follicles still reside in the germarium at eclosion.

A second class of GSC-related clones was termed CB clones (Figure 2B). CB clones were recognized as single 16-cell labeled cysts located ~5 divisions downstream from unlabeled GSCs. They are predicted to result from segregation of the lineage marker gene into the CB daughter rather than the GSC daughter at the first division of a recombined GSC (Figure 1F). Across all time points, we observed 199 CB clones and 221 GSC clones. The closeness of these numbers to 50:50 segregation limits the role of GSC symmetric division plays in filling early niches. As predicted, CB clones were located on average more distal than the oldest cyst in marked GSC clones.

Characterization of direct-developing wave 1.5 follicles providing early fertility

The most common clonal pattern was partial labeling of 8 or fewer germ cells in a single follicle. Such clones result from recombination within a direct developing PCG or a downstream cyst cell, and therefore mark wave 1.5 follicles (Figure 1E, 2E; Table S3). Rarely, wave 1.5 follicles contained 16-cell clones due to prior symmetric division of a recombined PGC (Figure S2B) before

it began direct cyst formation (Figure 2F). Partially labeled wave 1.5 cysts were also observed in germarium region 2b (Figure 2F) and S1, posterior to the oldest wave 2 cysts.

Comparing the labeling pattern of wave 1.5 follicles across time points, we found that the youngest wave 1.5 follicles increased their labeling frequency coincident with the 10h APF ecdysone pulse, whereas the two most mature follicles had already undergone more cyst divisions and responded less (Figure 2G). Averaging all wave 1.5 follicles at a given time point, a steady decline in the percentage of PGC labeling (8-cell clones) was seen as a function of clone induction times, indicating the timing of initial PGC cyst divisions (Figure 2H). In contrast, there was a steady increase in the percentage of cysts undergoing successively later rounds of cyst division. These data show that wave 1.5 cyst divisions proceed at a similar average speed, with 67% remaining as undivided PGCs at -2h whereas only 33% of clones marked PGCs that have not yet begun cyst divisions at 14h.

Since all germline cysts and follicles within ovarioles at eclosion are derived from either GSCs (wave 2) or direct-developing PGCs (wave 1.5), we quantified wave size. On average, each ovariole contains 12.5 wave 2 cysts (5 cysts produced per GSC and 2.5 GSCs per ovariole, n=165). Likewise wave 1.5 was responsible for about 6.5 follicles per ovariole (Figure 2D). Thus, ~100 wave 1.5 follicles are produced per ovary, a much larger population than previously estimated.

A large, novel population of wave 1 germ cells turns over between 22h-26h APF

Direct examination of pupal ovaries from -2h to 30h APF allowed us to further study developing wave 2 and wave 1.5 follicles, and revealed an unexpected third follicle wave that we term “wave 1” (Figure 3A-J). The number of single germ cells plus cysts (wave 2 and wave 1.5) in each ovariole was determined based on fusome morphology beginning at 6h (Movie S2). It continues to increase past 10h, past the time when ovarioles become defined by the sheath (Figure

3D) until 18h (Figure 3K). This proliferation results from the last round of PGC symmetric division in ovarioles, which was last observed in 18h ovaries. Lack of GSC division during this time confirms this conclusion (Figure 2C).

Beginning as early as 6h (Figure 3D), a subpopulation of PGCs was observed to migrate toward the posterior of the ovary. Posterior somatic cells form a conical structure at this time (Figure 3E-F, L). Germ cell posterior movement continued, producing a distinct group (Figure 3F-G, L, arrows). The germ cells at the posterior further increase in number as they form cysts and by 22h they aggregate to form a mass of approximately 150 cells (Figure 3G-H, L; Figure 4D, orange line). Between 22-26h APF, all the posterior germ cells and some adjacent somatic cells are extruded from the ovary posterior (Figure 3I). We term these cyst structures "wave 1" because of their early development and atresia-like turnover, akin to wave 1 follicles in the mouse. All three waves are visible along the A-P axis in Figure 3H. By 30h, the ovary has completely lost wave 1 germ cells and its protruding posterior, appearing spherical in shape and has been repaired (Figure 3J).

In 10h ovaries, clear vacuoles appear around germ cells (Figure 3E, M, N), coincident with the small prepupal ecdysone pulse (Figure 1A). Smaller vacuoles were observed inside germ cells, confirming germ cells to be the origin for such vacuoles (Figure 3N-N'). These vacuoles disappeared within 4 hours without causing lasting morphological changes to the tissue (Figure 3F).

Rapid proliferation and clearance of wave 1 germ cells

We analyzed lineage-labeled germ cells directly in pupal ovaries 24 hours after clone induction to gain further insight into wave 1 development. Analyzing clones induced at -2h and 2h in pupal ovaries 24 hours later showed that individual wave 1 clones typically contained multiple nearby cysts that were fully labeled (Figure 4A-C), indicating wave 1 precursor PGCs expand rapidly by symmetric division and then by forming germline cysts with typical fusomes. 1B1 staining reveals

branched fusome structure that is indicative of cyst division stage. Viewing the ovary from the posterior reveals branched 8 or 16-cell fusomes in >10 remaining wave 1 cysts (Figure 4B-B'). Adjacent fully labeled cysts suggest they originate from a single PGC labeled 24 hours ago (Figure 4C-C'). We estimated the cumulative total number of wave 1 germ cells released by first determining that at 18h APF when wave 1 cyst number reaches the maximum, there are 22 wave 1 cysts of various sizes indicated by fusome structure (Figure 4D, S2D, S2E). At this time before cells began to be extruded, only 15% of cysts contain 16 cells (Figure 4D, blue line). However, at 22h and 26h APF the percentage of 16-cell cysts among the remaining wave 1 cysts continued to rise and reached 75%, indicating continuous cyst division even though the total number of wave 1 cells starts to fall due to ongoing cell extrusion (Figure 4D). Taking into account the simultaneous proliferation and extrusion, we estimate that in total between 250-350 wave 1 germ cells are expelled. Clusters of wave 1 germ cells and associated somatic cells break off in groups at the posterior (Figure 4E-G).

Immediately before and as wave 1 germ cells exit the ovary, large spherical vacuoles with significant BODIPY-stainable lipid droplet enrichment appear around them, likely derived from these germ cells (Figure 4H-H'). We examined 22-26h APF testes as well, and found a similar sequence of regional germ cell appearance changes (Figure 4I-I') followed by expulsion from the gonad (Figure 4J-L) with concurrent lipid droplet accumulation (Figure 4K', L'). In the testis, however, cells were lost from the sides of the gonad rather than the posterior, where germ cells are absent. This indicates that germ cell extrusion is not a female-specific process, and may serve a more general purpose in development. Wave 1 extrusion temporally overlaps with the 24h APF pharate adult ecdysone pulse, along with the observed release of lipid-rich vacuoles, hints at a causal relationship between these events.

<u>Ovarioles contain two pupal FSCs that resemble adult FSCs</u>

In normal adult ovarioles, two long-lived FSCs each stably associate ($t_{1/2}$ ~20 days) with a separate niche located on opposite sides of the germarium at the 2a/2b junction. Adult FSCs divide alternately to supply a follicle founder cell to each passing germline cyst as cysts lose their covering of escort cell membranes. The two FSC-derived founder cells continue dividing to produce 50% of the continuous follicular monolayer comprising 60-80 cells in about 48 hours, that is sufficient for follicle budding, including polar and stalk follicle cells. Electron microscopy (King et al., 1968) and our observations (Figure S1C) show that early pupal ovarioles at least up to 40h APF lack a distinct 2a/2b junction. Consequently, it was unclear where pupal FSCs are located or if follicle cells generated during pupal stage arise in a different manner than adults.

Lineage analysis of clones induced at -2h, 2h or 6h scored at eclosion revealed very few FSC clones, defined as clones labeling multiple follicle cells on multiple successive follicles (Figure 5A). However, starting at 10h APF, adult-like clones that define a pupal FSC population ("FSC-P") began to be observed more frequently (Figure 5B). The longest FSC-P clones initiated at precisely the same position at the 2a/2b junction described for the location of adult FSCs. Like adult FSC clones, follicle cells in FSC-P clones were labeled in largely contiguous patches on adjacent follicles. However, most FSC-P clones spanned a group of adjacent follicles posterior to the 2a/2b junction (Figure 5C-C', D), identical to adult FSC clones whose stem cells had been replaced by an unlabeled FSC. As there was no disruption of follicle production, these FSC-P clones likely were also terminated earlier by displacement at the region 2a/2b niche. However, the frequency of FSC-P displacement was much higher than in adult FSCs. We measured the frequency of replacement points at different follicle positions along the ovariole by recording the start and end point of FSC-P clones that did not span the entire range. Significantly more clones contain such boundaries on the earliest wave 1.5 follicles (which develop to later stages by the time of study), showing that FSC-P

instability drops sharply with time (Figure 5E). Measurements of the follicle surface using 3D reconstruction showed that FSC-P clones label an average of about 49% of follicle surface area (Figure 5G, G', H; see also Movie S3-S4). This indicates that two founder cells per follicle, produced from FSC-Ps, as in adults, generate the follicular layer on wave 1.5 follicles during pupal stage (except for the oldest wave 1.5 follicle, see below).

The first wave 2 follicle activates a new set of FSCs

A second class of FSC clones was observed to arise much later in pupal development. They initiate at the 2a/2b junction, but have only produced follicle cells for 1-3 subsequent cysts (Figure 5F). These were termed "FSC-A" (adult FSC) clones since their span closely matched the location of the oldest wave 2 adult cysts, and they remained active following eclosion. To compare their relatively location, we measured the location of CB clones which mark initial wave 2 follicles and compared it with the most distal cysts marked by FSC-A clones. >75% of CB clones are found at the first or second region 2b cyst, and less frequently at the S1 follicle (Figure 5I). This indicates that the first wave 2 cyst passes the 2a/2b junction, and moves 1-3 additional cyst positions downstream. Notably, the average distribution of FSC-A clone end points closely matched the CB clone distribution (Figure 5I). In addition, the FSC-P clones that had most recently lost their FSC showed a very similar distribution of loss point to FSC-A and CB clones (Figure 5C', I). This suggests that losses of FSC-P in the germarium region are often caused by FSC-A displacement, which may account for the small peak at this position in the FSC-P loss rate (Figure 5E).

To precisely correlate FSC-P replacement by FSC-A, we analyzed rare ovarioles in which both the first wave 2 cyst and one of the FSC types were lineage labeled. CB clones located at the first R2b position were co-labeled with FSC-A clones that did not extend beyond that cyst (Figure 5J). FSC-P clones were also observed to end immediately before the advent of a CB clone when these

two types of clones are labeled in the same ovariole (Figure 5K); and when a CB clone has not yet reached the 2a/2b junction, the co-labeled FSC-P clone retained its active FSC at 2a/2b junction (Figure 5L). These double clones strongly support the model that FSC-As replace FSC-Ps upon the advent of the first wave 2 cyst, and FSC-As produce coverage for wave 2 follicles while FSC-Ps produce coverage for wave 1.5 follicles.

The first wave 1.5 follicles have unusual properties

Follicular coverage of the first wave 1.5 follicles in each ovariole included contributions from a different source in addition to FSC-Ps. Terminal wave 1.5 follicle cell clones frequently contain labeled follicle cells in a posterior patch and less often in other positions (Figure S3G-G'). Basal stalk cells were previously reported to contribute to pupal follicle cells (Reilein et al. 2021), and movement of basal stalk cells onto the posterior wave 1.5 follicle layer provides an attractive explanation for the bias terminal follicle clones show toward the posterior region where the stalk attaches. Similar behavior is also documented in the adult ovarioles, where inter-follicular stalk cells are known to sometimes offload extra cells onto the adjoining follicle (Nystul and Spradling, 2010).

The oldest 1-2 wave 1.5 follicles also at low frequency manifested small developmental changes compared to normal adult follicles. We observed examples with oversized polar cells, suggesting increased polyploidization (Figure S2F). The number and size of border cell clusters, which include the anterior polar cells were sometimes enlarged and delayed in migration (Figure S2F-G). Initial wave 1.5 follicles also had a higher frequency of germline cyst developmental abnormalities where they contain 8 or 32 cells per follicle(Figure S2H), indicating they underwent one less or one more round of cyst division.

Cap cell and escort cell differentiation correlates with niche development

Clones were also recorded of cap cells (CC) and specific escort cells (EC) clones (Figure 5A) that could be recognized by location (Figure S4A, K). EC1-3 locate around the GSC niche, and EC4-6 are close to FSC niches. An EC1 wraps the surface of each GSC, while behind it lies EC2 (Figure S4B-C). A median EC3 is also present between the GSCs (Figure S4D). Three ECs similarly surround both FSC niches (Gao et al., 2019; Rust et al., 2020). EC4 is on the surface of germarium and directly contacts the FSC (Figure S4E), more anterior to it is EC5 (Figure S4F). Another median EC type, EC6, is found between the two FSCs located internal in the germarium (Figure S4G). At least in some cases, EC6 cell membranes extend to an adjacent FSC (Sahai-Hernandez and Nystul, 2013).

The labeling frequencies of these clones increased at 10h APF (Figure 5A). Since these clones were usually single cells, or in very small groups (Figure S4I), it suggests that ECs and CCs may undergo their final division(s) around 10h APF. Observed EC clone sizes confirm they divide minimally after 10h, as 99% of EC clone contain 4 or fewer cells, and 52% contain only one EC. 84% of CC clones were single-cell clones, with the rest containing 2 cells (Table S2). The increase was greater for EC1 and EC2, the most anterior ECs next to the GSC niche, than for other ECs. Since CC clones also showed a similar increase (Figure 5A), this argues that the completion of GSC niches happens at this time.

DISCUSSION

Drosophila females produce three waves of follicles

Our experiments demonstrated that the well-studied GSC-based system of follicle production in Drosophila (wave 2) is preceded by two earlier follicle waves. Wave 1.5 and wave 1 follicles directly derive from PGCs which expand to a final population of 160 PGCs by 18h APF (Figure S2A). Previously, it was thought that larval PGCs not established as GSCs only produced the first

30-60 eggs with identical properties as later eggs (Zhu and Xie, 2003; Asaoka and Lin, 2004). In addition to a larger number of larval PGCs, we documented ongoing PGC proliferation up to 16h APF and showed they support wave 1 and wave 1.5 development (Figure 3K).

Exactly how many PGCs are needed to produce the 40 GSCs observed (2.7 per ovariole) is not yet precisely known. Our extensive characterization of labeled GSC clones did not enable us to fully test the prediction that the first GSC to enter a niche expands symmetrically (Zhu and Xie, 2003). We found that after an initial GSC division, instead of both daughters remaining in the niche, as expected if empty sites were present, the labeled daughter left the niche entirely nearly half the time to produce a CB clone. This indicates that initial niches lack room to support symmetric division, because like adult niches, any space is rapidly filled with a germ cell. Consistent with that conclusion, we observed continued production of the niche component cap, EC1 and EC2 cells, likely allowing the GSC niches to keep growing in size and admitting new stem cells until at least 10h APF. Estimates of when GSCs begin asymmetric divisions have varied (Zhu and Xie, 2003; Song et al., 2007; Banish et al., 2021). We found that the 10h ecdysone pulse correlates with increased numbers of bam-expressing germ cells and GSC division, but most bam-positive germ cells still reside at the end of the ovarioles, due to PGC direct differentiation into early wave 1.5 cysts. GSCs go on to produce about 5 daughter cysts each by the time of eclosion which remain within the germarium.

<u>The ovary prioritizes rapid production of more than 100 wave 1.5 follicles</u>

Our studies argue that wave 1.5 follicles are intrinsically important, rather than just products of excess PGCs needed to ensure that GSC niches are filled. The PGCs posterior to GSC niches expand by symmetric division (Figure S2B) and directly develop to produce this wave, enough to ensure that all follicles and ~1-2 posterior cysts per ovariole at eclosion are of wave 1.5 origin. 33% of wave 1.5

PGCs begin cyst formation in the larval ovary and move toward its posterior. The growing number of developing wave 1.5 follicles is responsible for most germ cell bam expression in the middle of the ovary, especially after 10h APF (Figure 3B-E). Wave 1.5 follicles are produced unusually fast. During the 96 hours of pupal development, wave 1.5 PGCs produce nearly mature follicles at the end of each ovariole. These wave 1.5 follicles will have developed from PGC to mature egg in a little more than 5 days. In contrast, adult CBs require 7-8 days to complete oogenesis (King, 1970; Lin and Spradling, 1993). Despite their rapid production, the defects we observed in a minority of only the most rapidly produced terminal wave 1.5 follicles probably are too rare to have much impact on reproduction.

Exceptionally rapid development is one of several indications that wave 1.5 follicles are functionally important. Their follicular covering is produced by a different set of stem cells, FSC-P, than wave 2 follicles, which use FSC-A. Wave 1.5 follicles are less dependent on adult nutrition than wave 2 follicles, because they can acquire sufficient yolk from larval nutrients stored in the fat body. In contrast, wave 2 follicles have not yet left the germarium at eclosion, and their maturation depends almost entirely on finding environmental nutrient sources. Thus, under the limited nutrient conditions most females confront in the wild, at least some wave 1.5 eggs but often no wave 2 eggs will be completed and ovulated. Therefore, wave 1.5 eggs may be specially adapted to limited environmental resources, and wave 2 eggs to nutrient-rich conditions. Our precise characterization of these two follicle waves will now facilitate a search for the molecular differences between wave 1.5 and wave 2 eggs, and between their distinct populations of follicle cells. Differentially expressed genes in FSC-P compared to FSC-A daughter cells might indicate what genetic, molecular and physiological differences facilitate adaptation to different nutrient conditions.

<u>Drosophila wave 1 follicles may contribute to pharate adult ecdysone pulse</u>

Our finding that an early Drosophila germ cell wave produces 250-350 germ cells in germline cysts that turn over between 22h and 26h APF strongly suggests these wave 1 follicles have a function other than gametogenesis. Wave 1 germline cysts are extruded from the ovary together with a group of somatic cells that forms a conical structure at the posterior (Figure 3L), potentially acting synergistically to enable such process to take place. Swarm cells, a population that migrates to the posterior ovary region during L3 associate with wave 1 cysts and may constitute the somatic cells extruded along with them. It is possible that swarm cell migration evolved to support wave 1 function, and swarm cells that are not extruded are not detected in the adult ovary.

Our study shows that wave 1 cells do not represent an obsolete larval structure to be turned over during metamorphosis, but instead are a new cell population produced in a highly programmed manner with rapid proliferation shortly before collective turnover. Wave one turnover occurs at the onset of the pharate adult ecdysone pulse that is critically important for pupal metamorphosis, the source of this pulse was previously proposed to be an unidentified tissue releasing ecdysone recycled from earlier times in development and stored in an inactive form (Scanlan et al., 2021). Wave 1 germ cells in the ovary, and a similar group of germ cells in the testis at the same time both turn over as lipid-enriched vacuoles appear around them, suggesting this is not a female-specific process and may have a general purpose during development. We propose that wave 1 follicles contribute to ecdysone production, either by storing and releasing ecdysone, or indirectly by signaling to other tissues responsible for the release. Determining the true function of transient wave 1 follicles will ultimately require a separate study that is now possible based on their properties reported here.

<u>How similar are the three follicle waves in Drosophila to those in mice?</u>

The general similarity of the three Drosophila follicle waves described here to those found in the mouse ovary was surprising. It is well established that wave 2 follicles in both species provide

the major mechanism to produce large numbers of eggs for sustained fertility through adulthood. Wave 1 in both species undergo programmed turnover, and wave 1.5 follicles provide the earliest eggs for fertility. The turnover of wave 1 temporally overlap with critical hormone pulses mediating adult development in both species, while mouse wave 1 clearly plays a role in androgen production, during peri-puberty. Further experiments are needed to clarify Drosophila wave 1 function.

There are many differences between the waves in Drosophila and mouse that suggest they could also have arisen independently in evolution. Wave 2 uses stem cells in Drosophila but follicle quiescence in the mouse to sustain fertility. Wave 1.5 produces about 110 follicles in Drosophila but more than 400 in mouse to generate the first progeny. The "atresia" program of wave 1 differs between these species. Drosophila wave 1 undergoes atresia at an earlier stage of follicle development, possibly also associating with a novel somatic cell type. Further study and comparison of the genetic pathways used by wave 1 germline and somatic cells in both species will likely provide insight into both the mechanisms and similarities between Drosophila and mouse waves.

Drosophila pupal ovarian FSCs offer insight into stem cell niche development

The behavior of stem cell niches represent an important aspect of stem cell biology, including homeostatic tissue maintenance and aging (Morrison and Spradling, 2008). We identified pupal FSCs and showed that precisely 2 FSC-Ps reside in niches comprised of cells located at the 2a/2b junction in newly eclosed ovarioles, the location of adult FSCs. FSC-A stem cells reside at this same location. The precise cellular anatomy and regulation of pupal niches can now more easily be characterized by manipulating candidate pupal cells and assessing the effects on the behavior of clonally marked FSC-P and FSC-A clones.

The replacement of two FSC-P stem cells in each ovariole by two new FSC-A stem cells associated with the switch from wave 1.5 cysts to wave 2 cysts provides one of the clearest examples

of developmentally programmed stem cell replacement. Previously, stem cells were shown to be capable of replacement when their adhesion to a niche was greater than the adhesivity of the current resident stem cell. It is less clear, however, how or why such stem cell replacement would take place. The mechanism by which the initial wave 2 cyst induces stem cell replacement would be of particular interest. The most plausible mechanism would be if early wave 2 cysts carried FSC-competent progenitor cells with higher adhesivity than FSC-Ps. As the first wave 2 cyst passes the 2a/2b junction, such cells would come into contact with the niches and induce replacement.

The dramatic 5-fold increase in FSC-P stability in its niche during early wave 1.5 development (Figure 5E) also presents an opportunity to better understand the initial formation of stem cell niches. Each FSC niche houses only a single stem cell defined by a few niche cells, the simplicity makes it an attractive model. Adult FSC maintenance by multiple common long-range intercellular signals is well-characterized (Sahai-Hernandez and Nystul, 2013). Thus, it should be possible to determine which developmental parameters are responsible for this initial FSC niche instability causing frequent pupal FSC replacement.

MATERIALS AND METHODS

Fly Husbandry and Developmental Staging

Flies were cultured in 25ºC incubators on standard cornmeal/molasses/agar media, therefore all APF hours mentioned are measured at 25ºC. To collect pupa with accurate APF timing, immobile wandering third instar larva are collected, and 4 hours later only the larva that underwent pupariation are retained while those that are still larva are discarded. This method ascertains that all the remaining pupa to be examined have pupariated at the same time within a $\pm$2 hour window. The X-15-29 and X-15-33 fly lines used for lineage tracing were from Dr. Norbert Perrimon, and the bamP-GFP fly line was from Dr. Mark Van Doren. We used FlyBase (FB2025_05) to find information on

phenotypes/function/stocks/gene expression/orthologs etc. Genetic nomenclature also follows Flybase (Öztürk-Çolak et al. 2024).

Lineage Tracing Design

Lineage clones from mitotic recombination were generated using heat shock by the method of Harrison and Perrimon (1993). Females of genotype X-15-33/X-15-29; MKRS, hs-FLP/+ were generated by standard crosses. To induce flippase expression, larva/pupa at various developmental times as specified in the results were heat shocked at 37°C by immersion in a circulating water bath for 1 hour. The recombination enabled by flippase constructs a functional copy of α84Btubulin-LacZ, leading to LacZ reporter being constitutively expressed in the cell where recombination happened. The LacZ-marked clone produced by proliferation of the labeled individual cells in the ovary were subsequently imaged either 24 hours (in pupae) or 5 days (in newly eclosed adult) after heat shock. Quantification of cells in lineage clones was done in Imaris by examining across the entire Z-stack of tissue.

Immunostaining and Light Microscopy

Drosophila pupal and adult ovaries were dissected in phosphate-buffered saline (PBS) followed by immediate fixation in 4% paraformaldehyde in PBS (made from stock 16% Paraformaldehyde Aqueous Solution EM Grade, Electron Microscopy Sciences, SKU#15710) for 30 minutes at room temperature on rocking platform. Samples were then washed and permeabilized twice with 1% PBT (Triton X-100 in PBS) at 10 minutes each, blocked in 1% PBTB (0.6% BSA and 5% NGS in 1%PBT) overnight at 4°C, and incubated with primary antibodies in 0.3% PBTB (0.6% BSA and 5% NGS in 0.3%PBT) overnight at 4°C. Next, samples were washed 2 times with 0.3% PBT and 1 time with 0.3%PBTB at 30 minutes each. Secondary antibodies were then added in 0.3% PBTB and incubation was done overnight at 4°C, then samples were washed 3 times with 0.3% PBT,

the second time including 1:10,000 DAPI if nuclear stain was desired. Lastly, the sample was briefly washed in PBS before mounting on slide in Vectashield Antifade mounting medium. All overnight incubations were performed on a platform rocker and other shorter incubations on a nutator.

Primary antibodies used were GFP (1:200, chicken, Abcam Ab13970), LacZ (1:200, chicken, Abcam Ab134435), vasa (1:50,000, rabbit, from Dr. Ruth Lehmann) and 1B1/hts (1:50, mouse, from Developmental Studies Hybridoma Bank). Secondary antibodies used were Invitrogen AF-488, AF-568 and AF-680, all at 1:250. Images were acquired on Leica TCS SP8 confocal microscope, using 10X/NA0.25 objective for ovarioles and 63X/NA1.4 objective for germaria and pupal ovaries.

Image Analysis and Cell Quantification

Z-stack images acquired were re-constructed into 3D object using Imaris software (v10.0.0). Statistical analysis of cells was conducted using the spot function with manual spot assignment and automated quantification. Lineage tracing clone size was determined based on the number of nls.GFP+ nuclei, and PGC/cyst number in the pupal ovaries was determined based on the number of 1B1+ spectrosomes/fusomes (sample shown in Supplemental Movie S2, a 6h APF pupal ovary with white circles showing spots assigned to each spectrosome/fusome).

DATA AVAILABILITY

Complete results from the lineage studies are included in the paper and Supplemental material. Original Z-stack images are available upon request.

ACKNOWLEDGEMENTS

ACS is an Investigator of the Howard Hughes Medical Institute which provided funding for this study. The authors are grateful to the Carnegie Institution for Science for hosting the Spradling laboratory and for long term support of its research. We thank Bhawana Maurya and Qi Yin for discussions and

many other members of the Spradling lab for useful comments on the manuscript. We also thank Mahmud Siddiqi for microscopy and software technical support.

REFERENCES

Asaoka M, Lin H. (2004). Germline stem cells in the Drosophila ovary descend from pole cells in the anterior region of the embryonic gonad. Development 131, 5079-89. doi: 10.1242/dev.01391.

Banisch TU, Slaidina M, Gupta S, Ho M, Gilboa L, Lehmann R. A transitory signaling center controls timing of primordial germ cell differentiation. Dev Cell. 2021 56:1742-1755.e4. doi: 10.1016/j.devcel.2021.05.008.

Byskov AG. 1974. Cell kinetic studies of follicular atresia in the mouse ovary. Journal of Reproduction and Fertility 37:277–285. DOI: https://doi.org/10.1530/jrf.0.0370277.

Camara N, Whitworth C, Dove A, Van Doren M. (2019). Doublesex controls specification and maintenance of the gonad stem cell niches in Drosophila. Development. 2019; 146: dev170001.

Clough E, Jimenez E, Kim YA, Whitworth C, Neville MC, Hempel LU, Pavlou HJ, Chen ZX, Sturgill D, Dale RK, Smith HE, Przytycka TM, Goodwin SF, Van Doren M, Oliver B. (2014). Sex- and tissue-specific functions of Drosophila doublesex transcription factor target genes. Dev Cell 31, 761-73. doi: 10.1016/j.devcel.2014.11.021.

Couderc JL, Godt D, Zollman S, Chen J, Li M, Tiong S, Cramton SE, Sahut-Barnola I, Laski FA. (2002). The bric à brac locus consists of two paralogous genes encoding BTB/POZ domain proteins and acts as a homeotic and morphogenetic regulator of imaginal development in Drosophila. Development 29, 2419-33. doi: 10.1242/dev.129.10.2419.

Dai J, Gilbert LI. (1991). Metamorphosis of the corpus allatum and degeneration of the prothoracic glands during the larval-pupal-adult transformation of Drosophila melanogaster: a cytophysiological analysis of the ring gland. Dev. Biol. 144, 309–326.

DeFalco T, Capel B. (2009). Gonad morphogenesis in vertebrates: divergent means to a convergent end. Annu Rev Cell Dev Biol. 25:457-82. doi: 10.1146/annurev.cellbio.042308.13350.

Diaz-de-la-Loza, M., R. P. Ray, P. S. Ganguly, S. Alt, J. R. Davis et al., (2018). Apical and basal matrix remodeling control epithelial morphogenesis. Dev. Cell 46: 23–39.

Eppig JJ, Handel MA. (2012). Origins of granulosa cells clarified and complexified by waves. Biol Reprod. 86(2):34. doi: 10.1095/biolreprod.111.096651.

Forbes, Z., Lin, H., Ingham, P. and Spradling, A.C. (1996). *hedgehog* is required for the proliferation and specification of somatic cells prior to egg chamber formation in Drosophila. Development 122: 1125-1135.

Gao, Y., Mao, Y., Xu, R. G., Zhu, R., Zhang, M., Sun, J., Shen, D., Peng, P., Xie, T., & Ni, J. Q. (2019). Defining gene networks controlling the maintenance and function of the differentiation niche by an in vivo systematic RNAi screen. Journal of Genetics and Genomics*, 46*, 19-30. https://doi.org/10.1016/j.jgg.2018.10.008.

Gilboa L, Lehmann R. (2006). Soma-germline interactions coordinate homeostasis and growth in the Drosophila gonad. Nature. 2006;443(7107):97–100. https://doi.org/10.1038/nature05068 PMID: 16936717

Godt D. and Laski FA. (1995). Mechanisms of cell rearrangement and cell recruitment in *Drosophila* ovary morphogenesis and the requirement of *bric à brac*. *Development* **121**, 173-187.

Harrison DA, Perrimon N. (1993). Simple and efficient generation of marked clones in Drosophila. Curr Biol. 3:424-33. doi: 10.1016/0960-9822(93)90349-s.

Jiang C, Baehrecke EH, Thummel CS. (1997). Steroid regulated programmed cell death during Drosophila metamorphosis. Development 124, 4673–83.

King RC, Aggarwal SK, Aggarwal U. (1968). The development of the female Drosophila reproductive system. J. Morphol. 124, 143-166. doi: 10.1002/jmor.1051240203.

King RC. (1970). Ovarian development in Drosophila melanogaster.

Kirilly, D., Wang, S. and Xie, T. (2011). Self-maintained escort cells form a germline stem cell differentiation niche. Developmen*t* 138, 5087-5097.

Kiss, I., A. H. Beaton, J. Tardiff, D. Fristrom, and J. W. Fristrom, (1988). Interactions and developmental effects of mutations in the Broad-Complex of Drosophila melanogaster . Genetics 118: 247–259.

Li, M. A., Alls, J. D., Avancini, R. M., Koo, K. & Godt, D. (2003). The large Maf factor Traffic Jam controls gonad morphogenesis in Drosophila. Nature Cell Biol. 5, 994-1000.

Lin H, Spradling AC (1993). Germline stem cell division and egg chamber development in transplanted germaria. Develop. Biol. 159: 140-152.

Margolis, J. and Spradling, A.C. (1995). Identification and behavior of epithelial stem cells in the Drosophila ovary. Development 121: 3797-3807.

Morrison SJ, Spradling AC. Stem cells and niches: mechanisms that promote stem cell maintenance throughout life. Cell. 2008 Feb 22;132(4):598-611. doi: 10.1016/j.cell.2008.01.038. PMID: 18295578; PMCID: PMC4505728.

Meinsohn MC, Hughes CHK, Estienne A, Saatcioglu HD, Pépin D, Duggavathi R, Murphy BD. (2021). A role for orphan nuclear receptor liver receptor homolog-1 (LRH-1, NR5A2) in primordial follicle activation. Sci Rep. 11(1):1079. doi: 10.1038/s41598-020-80178-4.

Mork L, Maatouk DM, McMahon JA, Guo JJ, Zhang P, McMahon AP, Capel B. (2012). Temporal differences in granulosa cell specification in the ovary reflect distinct follicle fates in mice. Biology of Reproduction 86:37. DOI: https://doi.org/10.1095/biolreprod.111.095208.

Nystul TG, Spradling A (2007). An epithelial niche in the Drosophila ovary undergoes long-range stem cell replacement. Cell Stem Cell 1, 277–285.

Nystul TG, Spradling A (2010). Regulation of epithelial stem cell replacement and follicle formation in the Drosophila ovary. Genetics 184, 505-515.

Panchal T, Chen X, Alchits E, Oh Y, Poon J, Kouptsova J, et al. (2017) Specification and spatial arrangement of cells in the germline stem cell niche of the Drosophila ovary depend on the Maf transcription factor Traffic jam. PLoS Genet 13, e1006790. https://doi.org/10.1371/journal.pgen.1006790.

Pazdernik N, Schedl T. (2013). Introduction to germ cell development in Caenorhabditis elegans. Adv Exp Med Biol. 757: 1-16. doi: 10.1007/978-1-4614-4015-4_1.

Reilein, A., H. V. Kogan, R. Misner, K. S. Park and D. Kalderon, 2021 Adult stem cells and niche cells segregate gradually from common precursors that build the adult Drosophila ovary during pupal development. Elife 10.

Rosales-Nieves AE, Marín-Menguiano M, López-Onieva L, Garrido-Maraver J, González-Reyes A (2025) ETS transcription factor pointed controls germline survival in Drosophila. PLoS Genet 21, e1011809. https://doi.org/10.1371/journal.pgen.1011809.

Rotgers E, Jørgensen, Yao HH-C (2018). At the crossroads of fate- somatic cell lineage specification in the fetal gonad. Endocrine Reviews 39(5):739–759.

Rust K, Byrnes LE, Yu KS, Park JS, Sneddon JB, Tward AD, Nystul TG. (2020). A single-cell atlas and lineage analysis of the adult Drosophila ovary. Nat Commun. 11, 5628- . doi: 10.1038/s41467-020-19361-0.

Rust K, Nystul T. (2020). Signal transduction in the early Drosophila follicle stem cell lineage. Curr Opin Insect Sci. 37: 39–48. doi:10.1016/j.cois.2019.11.005.

Sahai-Hernandez P, and Nystul TG (2013). A dynamic population of stromal cells contributes to the follicle stem cell niche in the Drosophila ovary. Development 140, 4490–4498.

Sahut-Barnola I, Godt D, Laski FA, Couderc J-L (1995). Drosophila ovary morphogenesis: analysis of terminal filament formation and identification of a gene required for this process. Dev Biol. 170, 127-35. doi: 10.1006/dbio.1995.1201.

Sahut-Barnola I., Dastugue B, Couderc J-L (1996). Terminal filament cell organization in the larval ovary of *Drosophila melanogaster*: ultrastructural observations and pattern of divisions. *Roux's Arch. Dev. Biol.* **205**, 356-363.

Scanlan JL, Robin C, Mirth CK. (2023) Rethinking the ecdysteroid source during Drosophila pupal-adult development. Insect Biochem Mol Biol. 152:103891. doi: 10.1016/ j.ibmb.2022.103891.

Schick J, Ermlich L, Kühl L, Hoffmann D, Raz E. (2025). Single-cell migration in development - Lessons from germ cells. Curr Top Dev Biol. 2025;164:1-27. doi: 10.1016/bs.ctdb.2025.01.002.

Shen W, Sun J. (2020.) Different modes of Notch activation and strength regulation in the spermathecal secretory lineage. Development. 147:dev184390. doi:10.1242/dev.184390.

Slaidina M, Banisch TU, Gupta S, Lehmann R. (2020). A single-cell atlas of the developing *Drosophila* ovary identifies follicle stem cell progenitors. Genes Dev. 34, 239-249. doi: 10.1101/gad.330464.119.

Slaidina M, Gupta S, Banisch TU, Lehmann R. (2021). A single-cell atlas reveals unanticipated cell type complexity in *Drosophila* ovaries. Genome Res. 31, 1938-1951. doi: 10.1101/gr.274340.120.

Song X, Zhu CH, Doan C, Xie T. (2002). Germline stem cells anchored by adherens junctions in the Drosophila ovary niches. Science 296, 1855-7. doi: 10.1126/science.1069871.

Song, X., G.B. Call, D. Kirilly, and T. Xie. (2007). Notch signaling controls germline stem cell niche formation in the Drosophila ovary. Development. 134:1071–1080. https://doi.org/10.1242/dev.003392

Trova S, Bovetti S, Bonzano S, De Marchis S, Peretto P. 2021. Sex steroids and the shaping of the peripubertal brain: the sexual-dimorphic set-up of adult neurogenesis. International Journal of Molecular Sciences 22:7984. DOI: https://doi.org/10.3390/ijms22157984, PMID: 34360747.

Wieschaus, E. and Szabad, J. (1979). The development and function of the female germ line in *Drosophila melanogaster*: A cell lineage study. Dev. Biol. 68, 29-46.

Xie T, Spradling AC (2000). A stem cell niche maintaining germ cell production in the Drosophila ovary. Science 290: 328-330.

Xu T, Jiang X, Denton D, Kumar S. (2020). Ecdysone controlled cell and tissue deletion. Cell Death & Diff. 27, 1-14.

Yaniv SP and Schuldiner (2016) A fly's view of neuronal remodeling. WIREs Dev Biol 2016, 5:618–635. doi: 10.1002/wdev.241

Yatsenko AS, Shcherbata HR. (2018). Stereotypical architecture of the stem cell niche is spatiotemporally established by miR-125-dependent coordination of Notch and steroid signaling. Development. 145, dev159178. https://doi.org/10.1242/dev.159178.

Yin Q, Spradling AC. (2025) Distinct waves of ovarian follicles contribute to mouse oocyte production. eLife, https://doi.org/10.7554/eLife.107352.1.

Zhang S, Wu S, Yao R, Wei X, Ohlstein B, Guo Z. (2024). Eclosion muscles secrete ecdysteroids to initiate asymmetric intestinal stem cell division in Drosophila. Dev Cell. 2024 Jan 8;59(1):125-140.e12. doi: 10.1016/j.devcel.2023.11.016.

Zheng, W., Zhang, H., & Liu, K. (2014). The two classes of primordial follicles in the mouse ovary: Their development, physiological functions and implications for future research. *Molecular Human Reproduction*, *20*(4), 286–292. https://doi.org/10.1093/molehr/gau007

Zhu C-H, Xie T. (2003). Clonal expansion of ovarian germline stem cells during niche formation in Drosophila. Development 130, 2579-2586.

FIGURE LEGENDS

Figure 1. Ovary anatomy and strategy for analyzing ovarian follicle waves.

A. Timeline of Drosophila development in hours after puparium formation (APF) and ecdysone levels during the third larval instar and pupal stages (modified from Scanlan et al., 2024). Red arrows show five clonal induction times; blue boxes show times of clone analysis. **B.** An ovariole from a fly heat-shocked at 2h APF is tipped with a germarium and 4 finished follicles. Its stage 8 follicle (S8) contains a clone labeling 4 of 16 germ cells. **C.** Germarium from a newly-eclosed fly heat-shocked at 2h APF. One lineage-labeled GSC and 4 progeny cysts are indicated. TF: terminal filament, CC: cap cells, EC: escort cells, FSC: follicle stem cell, FC: follicle cells. Fusomes: magenta (1B1). R1, R2a, R2b: germarium regions; S1: budding follicle. Scale bars: 50µm (B); 20µm (C.) **D.** Lineage labeling system. Heat shock (ΔT) activates a constitutive marker gene (green) in one daughter cell following mitosis (see Figure S1A.) **E.** Upper: Diagram of germline cyst formation from GSC, CB (cystoblast), 2-16-cell germline cysts (n-CC). Lower: clone size (green) following recombination at the indicated stages. **F.** Clone patterns induced by heat shock (ΔT) in a GSC. In GSC clone (above), N-1 daughter cysts are labeled; CB clone (below), the first daughter only is labeled.

Figure 2. Identifying wave 2 and wave 1.5 follicles.

A. GSC clone: LacZ-labeled GSC and 3 progeny cysts (arrowheads). **B.** CB clone: ovariole with single labeled 16-CC in R2B. **C.** GSC clone (blue) frequency (% ovarioles) vs induction time (hours APF). Clone size (orange), i.e. marked progeny number. N=346, 303, 129, 224, 164 respectively. Adult value from Margolis and Spradling, 1995. Mean +/- s.e.m. **D-D'.** Ovariole with all GSCs labeled, showing location of wave 2 and wave 1.5. D': Germarium region from D; all wave 2 (w2) cysts including 2 unlabeled cysts remain in germarium. **E.** Ovarioles with labeled w1.5 clones in

germ cells. **F.** Ovariole with fully labeled w1.5 follicle at S4-5 due to PGC symmetric division; a w1.5 follicle at S1 is magnified at right. **G.** Percentage of wave 1.5 follicles after the first cyst division at induction time points before 10h (blue) vs after 10h (tan), based on follicle order at eclosion (Stage 2-5 vs Stage 6-9). mean +/- s.e.m. across time points in each group. **H.** Percentages of wave 1.5 follicles PGCs and cyst stages versus times of clone induction showing progressive growth. Sample size for 2G and 2H are the same as in 2C. Scale bars are 20µm in A, B, D', 50µm in D, F, G.

Figure 3. Time course of pupal germ cell development in three follicle waves.

A. Schematic of a 10h APF pupal ovary oriented as in the following images, anterior to the left and posterior to the right. Arrows on top point to PGCs that become each of the three waves. **B-J.** A time sequence of pupal ovaries from -2h APF to 30h APF stained for germ cells (Vasa, red), forming cysts (bam-GFP, green), fusomes and somatic cell membranes (Hts/1B1, magenta) and nuclei (DAPI, blue). Arrowheads in D indicate newly formed ovarioles where ovariolar germ cells are separated by the sheath. Yellow arrows in F-G indicate the initial posterior wave 1 germ cell precursors. White arrows in E, H, I point to vacuoles devoid of antibody labeling that appear around wave 1 germ cells. The distinction of 3 waves is outlined in H. **K.** Quantification of total single PGCs and cysts per ovariole from -2h to 30h APF. Error bars represent SD across ovaries. n=10 ovaries for each time point. **L.** Stacked image of a 10µm section to show the large aggregation of all wave 1 germ cells into a disk-shaped mass in the posterior (arrow) of a 22h APF ovary. **M-N.** 10h APF germ cells magnified to show vacuoles and gaps between cells. Scale bars are 50µm in B-J and L, 10µm in M-N, N'.

Figure 4. Rapid proliferation of ovarian wave 1 germ cells and cysts.

A-A'. Pupal ovary lineage labeled at -2h APF and analyzed at 22h APF. Wave 1 germ cells at the posterior include lineage-labeled cysts with fusomes (A', arrows). **B-B'.** An ovary with the same

conditions as in 2A viewed from the posterior to reveal 14 wave 1 cysts, all with fusome (B'); 4 cysts are fully labeled. **C-C'.** Pupal ovary labeled at 2h APF and analyzed at 26h APF. A large segment of ovarian posterior region has broken off (upper right). C' shows that the cysts all have 16-cell fusomes, 3 are lineage marked in all cells. **D.** Quantification of wave 1 germ cells (orange) from the time they start to become spatially separated from the other two anterior waves (14h APF) until the time they have all been extruded from the ovary (30h APF). Points on dashed lines are cumulative total wave 1 germ cells ever produced discounting loss from extrusion and considering the continuous cyst amplification, as shown by the constant increase of 16 cell-cyst percentage out of all cysts in wave 1 (blue). n=10,12,12,9 ovaries, respectively. Error bars represent SD across ovaries. **E.** Pupal ovary labeled at 2h APF and analyzed at 26h APF showing significant germ cell extrusion from the posterior, among which two large clusters are lineage positive. **F-G.** 22h APF bamP-GFP fly line pupal ovaries showing germ cell extrusion similar to that seen in lineage tracing fly line ovaries. **H-H'.** 22h APF ovary with lipid-enriched vacuoles stained with BODIPY embedded in the ovary next to wave 1 germ cells. H' is the brightfield image of the same ovary showing morphology of the vacuoles (arrows). **I-I'.** A 22h APF testis with a large cluster of dying germ cells. I' shows the morphological change of this germ cell cluster under brightfield. **J.** A 22h APF testis showing significant amount of cell loss on the upper left corner. Areas in squares are magnified in K and L. **K-L.** Dying testical germ cells with remnant vasa expression. K' and L' show lipid enrichment similar to that of 4H. Scale bars are 50μm in all images.

Figure 5. FSC development correlates to follicle waves.

A. Somatic cell clone labeling rate as a function of induction times in hours APF. All cell types exhibit a marked increase in labeling rate at 10h. While FSC clones maintained the elevated rate, that of cap cell (CC) and escort cell (EC) clones dropped subsequently at 14h. n=621, 517, 449, 224, 459

total scored ovarioles. **B.** An FSC-P clone marked at 10h APF and analyzed by eclosion. Arrowhead points to the marked active FSC at 2a/2b junction. **C.** An FSC-P clone without a labeled active FSC, where the labeled FSC-P was replaced by an unlabeled FSC after its progeny has covered 4 sequential wave 1.5 follicles. **C'.** Germarium containing an FSC-P clone that does not contain an active FSC at 2a/2b junction (arrowheads). **D.** An FSC-P clone that lost its FSC early, only covering two early wave 1.5 follicles. **E.** Distribution of FSC-P clone loss points by follicle position. n=273 clones scored. **F.** A short FSC-A clone labeled at 14h APF that by eclosion has only covered two R2b cysts. **G-G'.** Example demonstrating how FSC-P follicle coverage rate was calculated in Imaris. G shows the raw signal, G' shows the clone coverage in blue and total FC layer on follicles with the clone in magenta. **H.** FSC-P follicle surface coverage rate calculated directly by surface area of the 3D objects created in Imaris, or by surface area converted from volume of such objects. n=26 follicles measured. **I.** Cyst location distribution of CB clones, FSC-A end points and FSC-P loss points. R2b+1 stands for the first R2b cyst position, etc. Only clones of these types that involve a position in R2b and S1 are recorded in the graph. n=130,54,40 clones for each clone type. **J.** Ovariole with an FSC-A clone surrounding a CB clone. **K.** Ovariole with a CB clone past the 2a/2b junction also containing an FSC-P clone that does not contain an active FSC, where the FSC-P loss point is immediately before the CB clone. **L.** Ovariole where a CB clone has not yet passed the 2a/2b junction also contains an FSC-P clone that has not lost its active FSC. Scale bars are 20μm in all images.

Fig.1

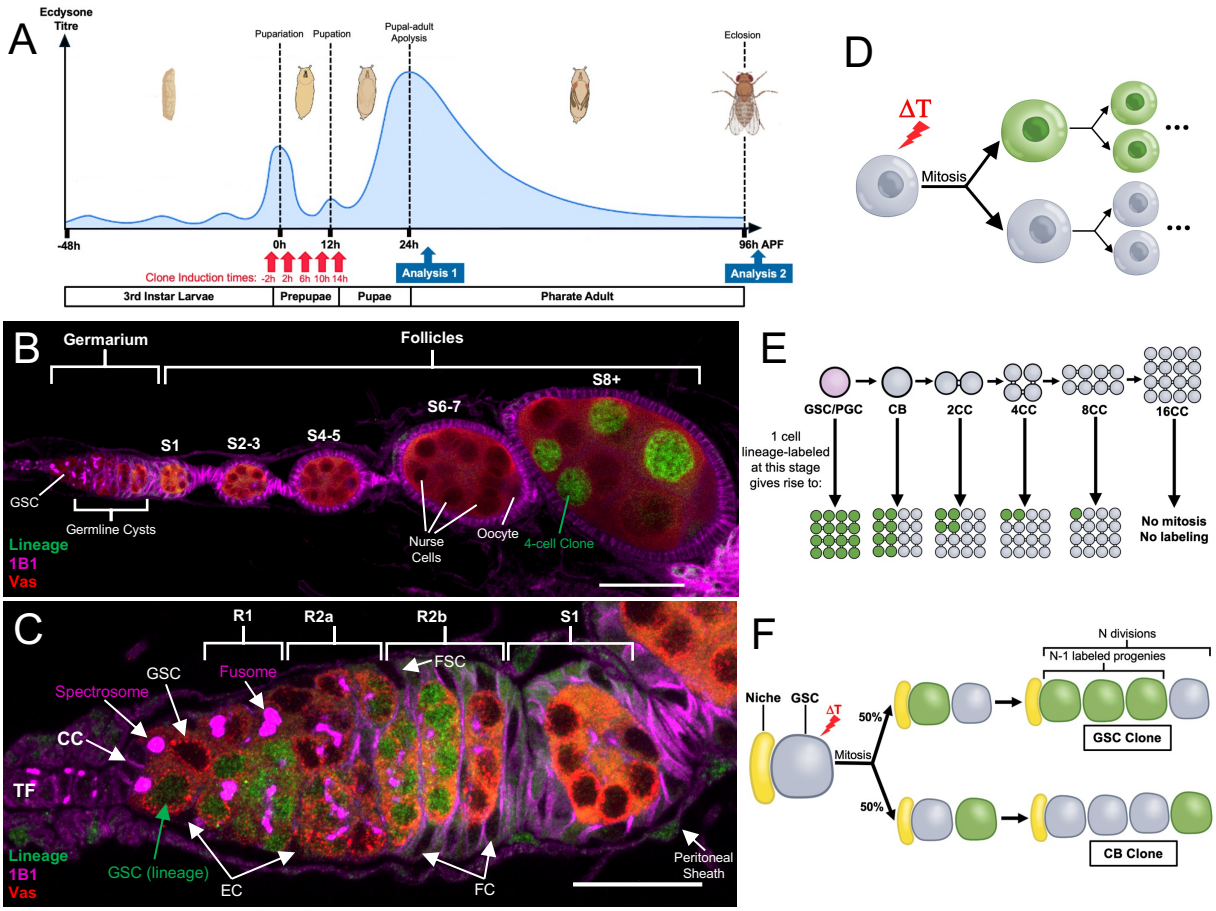
A
Ecdysone Titre
Pupariation
Pupation
Pupal-adult Apolysis
Eclosion
-48h
0h
12h
24h
96h APF
Clone Induction times: -2h 2h 6h 10h 14h
Analysis 1
Analysis 2
3rd Instar Larvae
Prepupae
Pupae
Pharate Adult
B
Germarium
Follicles
S1
S2-3
S4-5
S6-7
S8+
GSC
Germline Cysts
Nurse Cells
Oocyte
4-cell Clone
Lineage
1B1
Vas
C
R1
R2a
R2b
S1
GSC
Fusome
FSC
Spectrosome
CC
TF
GSC (lineage)
EC
FC
Peritoneal Sheath
Lineage
1B1
Vas
D
ΔT
Mitosis
E
GSC/PGC
CB
2CC
4CC
8CC
16CC
1 cell lineage-labeled at this stage gives rise to:
No mitosis
No labeling
F
N divisions
N-1 labeled progenies
Niche
GSC
ΔT
Mitosis
50%
50%
GSC Clone
CB Clone

Fig.2

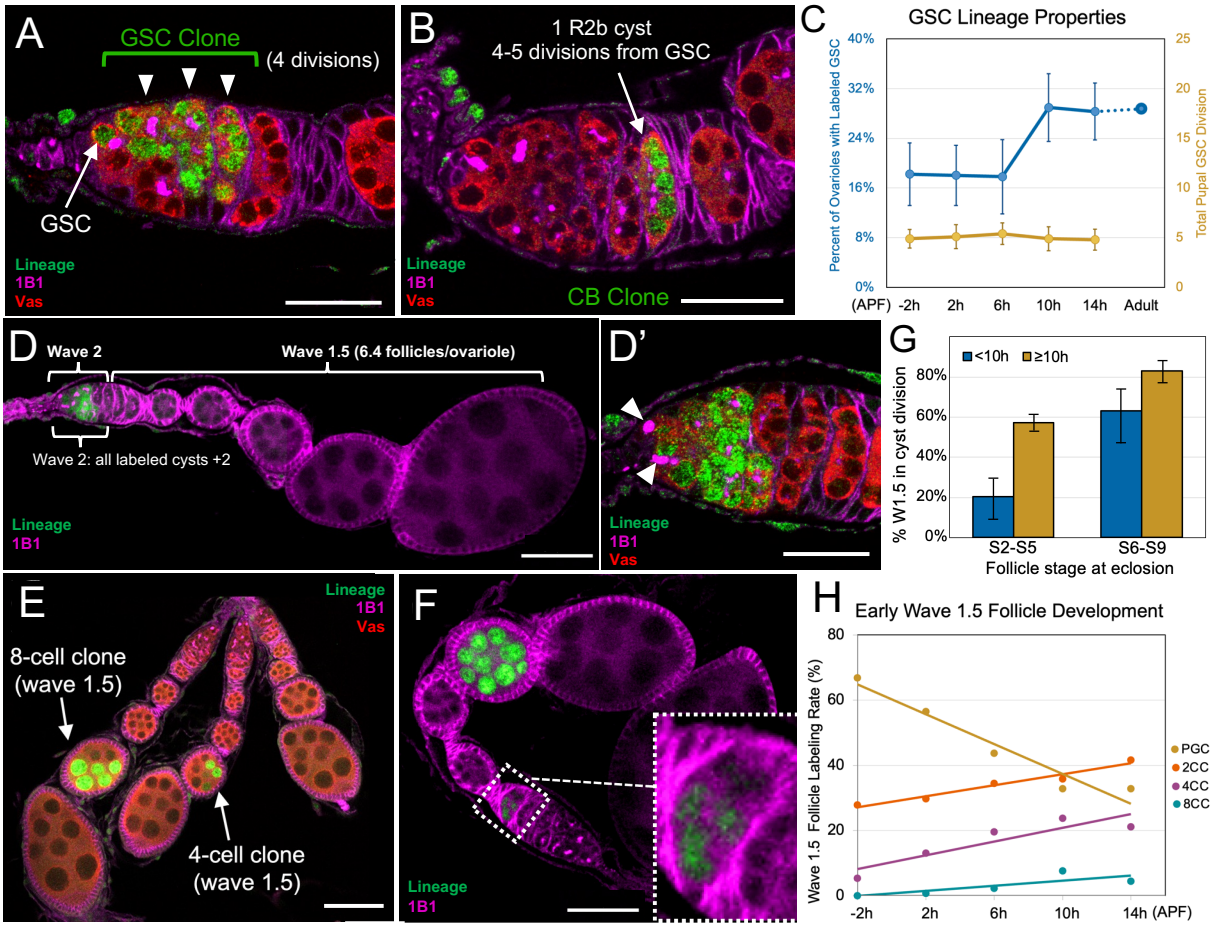
A
GSC Clone
(4 divisions)
GSC
Lineage
1B1
Vas
B
1 R2b cyst
4-5 divisions from GSC
Lineage
1B1
Vas
CB Clone
C
GSC Lineage Properties
Percent of Ovarioles with Labeled GSC
Total Pupal GSC Division
40%
32%
24%
16%
8%
0%
25
20
15
10
5
0
(APF) -2h
2h
6h
10h
14h
Adult
D
Wave 2
Wave 1.5 (6.4 follicles/ovariole)
Wave 2: all labeled cysts +2
Lineage
1B1
D'
Lineage
1B1
Vas
G
<10h
≥10h
% W1.5 in cyst division
80%
60%
40%
20%
0%
S2-S5
S6-S9
Follicle stage at eclosion
E
Lineage
1B1
Vas
8-cell clone
(wave 1.5)
4-cell clone
(wave 1.5)
F
Lineage
1B1
H
Early Wave 1.5 Follicle Development
Wave 1.5 Follicle Labeling Rate (%)
80
60
40
20
0
-2h
2h
6h
10h
14h (APF)
PGC
2CC
4CC
8CC

Fig.3

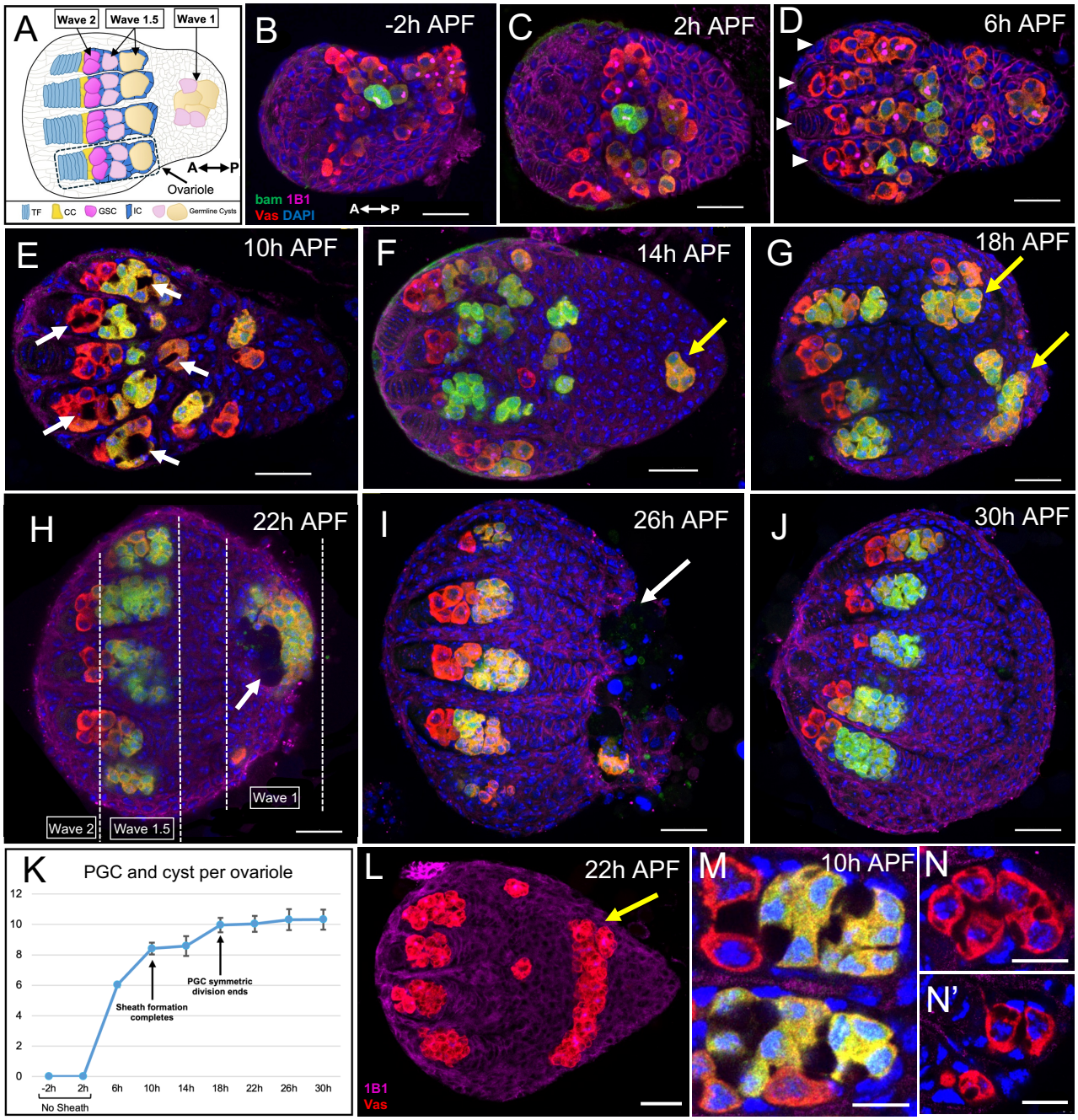
A
Wave 2
Wave 1.5
Wave 1
A↔P
Ovariole
TF
CC
GSC
IC
Germline Cysts
B
-2h APF
bam 1B1
Vas DAPI
A↔P
C
2h APF
D
6h APF
E
10h APF
F
14h APF
G
18h APF
H
22h APF
Wave 2
Wave 1.5
Wave 1
I
26h APF
J
30h APF
K
PGC and cyst per ovariole
12
10
8
6
4
2
0
-2h
2h
6h
10h
14h
18h
22h
26h
30h
No Sheath
Sheath formation completes
PGC symmetric division ends
L
22h APF
1B1
Vas
M
10h APF
N
N'

Fig.4

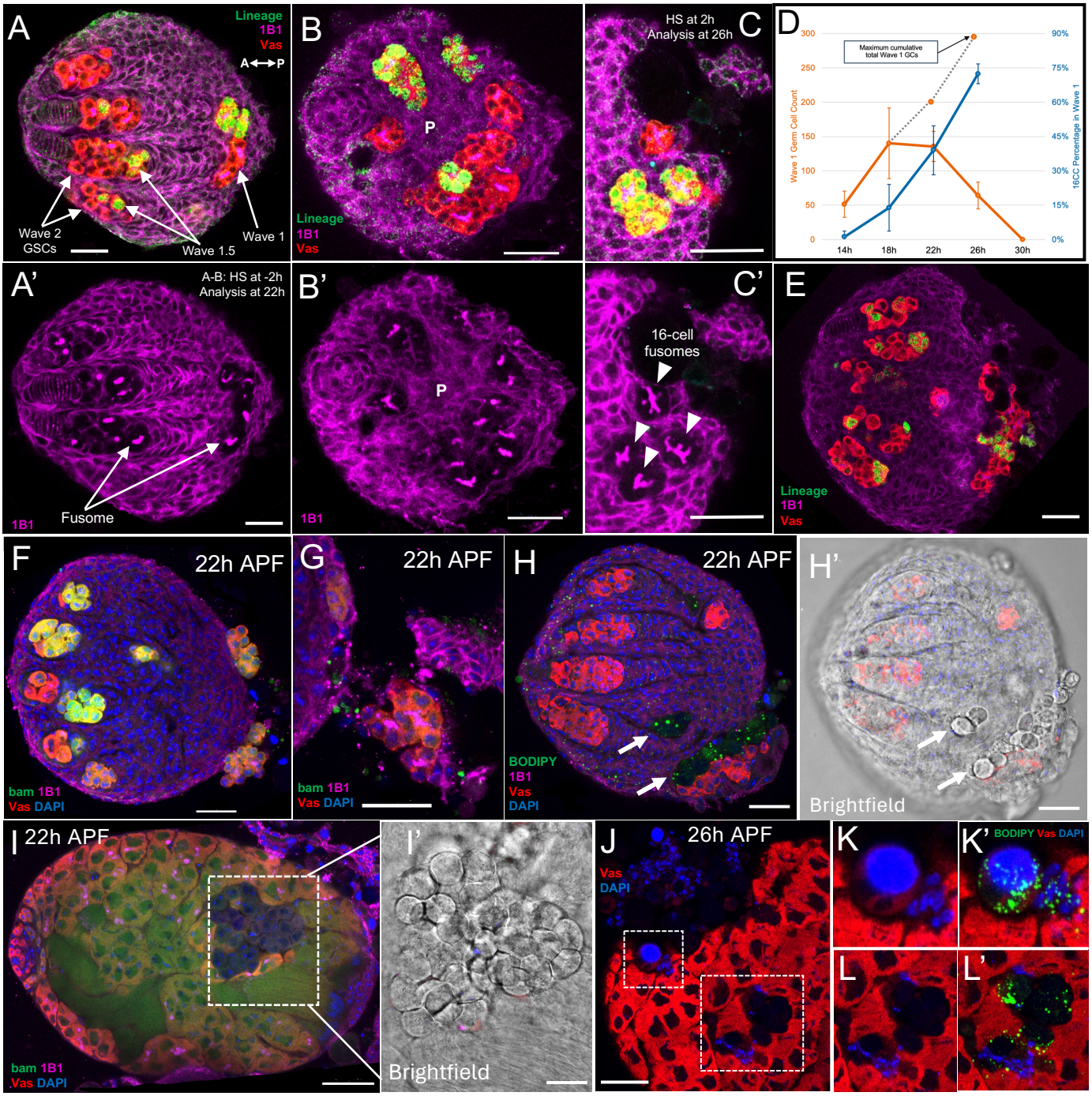
A
Lineage
1B1
Vas
A↔P
Wave 2
GSCs
Wave 1.5
Wave 1
B
P
Lineage
1B1
Vas
HS at 2h
Analysis at 26h
C
D
Maximum cumulative total Wave 1 GCs
Wave 1 Germ Cell Count
16CC Percentage in Wave 1
300
250
200
150
100
50
0
90%
75%
60%
45%
30%
15%
0%
14h
18h
22h
26h
30h
A'
A-B: HS at -2h
Analysis at 22h
1B1
Fusome
B'
P
1B1
C'
16-cell
fusomes
E
Lineage
1B1
Vas
F
22h APF
bam 1B1
Vas DAPI
G
22h APF
bam 1B1
Vas DAPI
H
22h APF
BODIPY
1B1
Vas
DAPI
H'
Brightfield
I 22h APF
bam 1B1
Vas DAPI
I'
Brightfield
J
26h APF
Vas
DAPI
K
K'
BODIPY Vas DAPI
L
L'

Fig.5

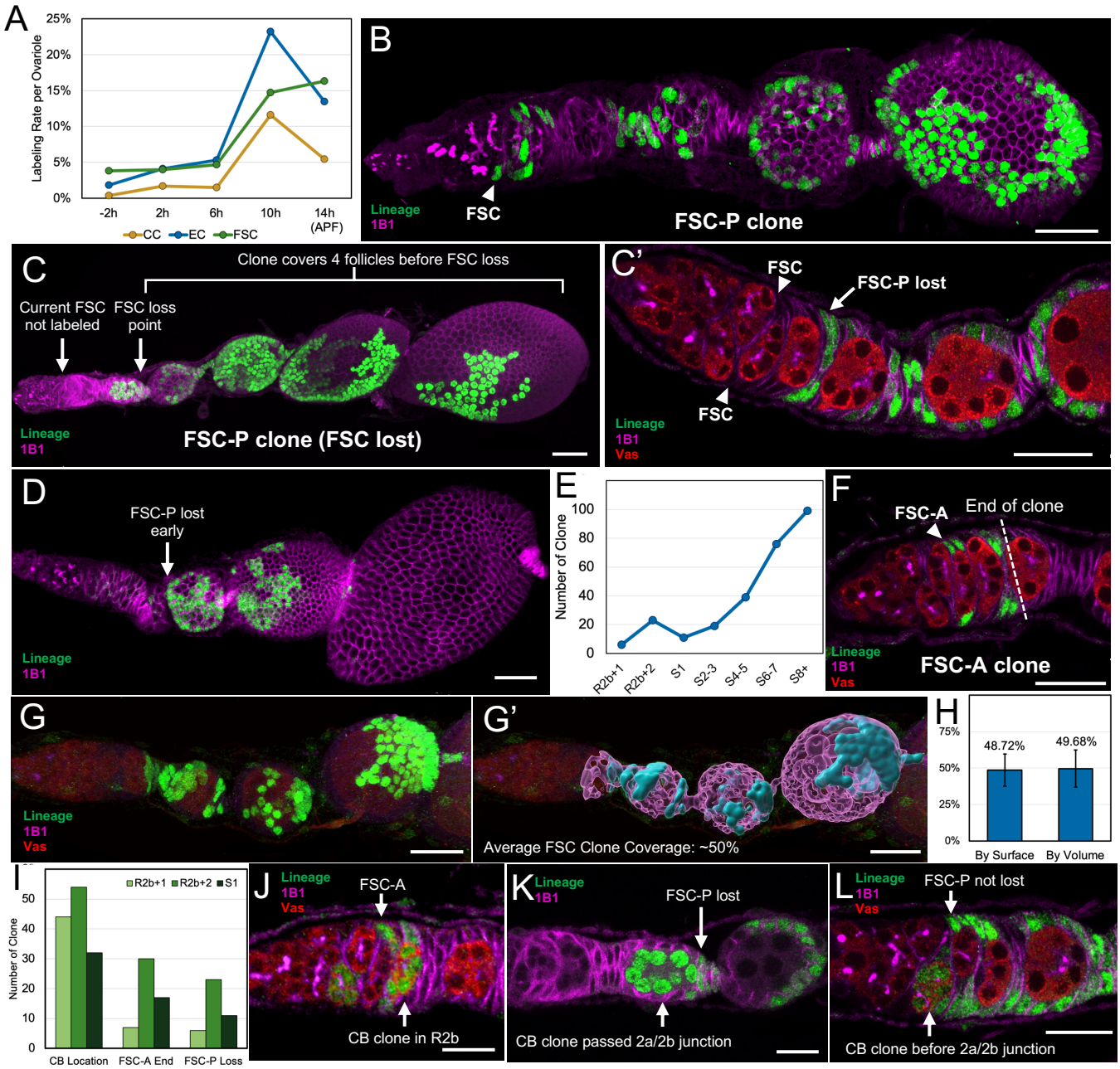
A
Labeling Rate per Ovariole
25%
20%
15%
10%
5%
0%
-2h
2h
6h
10h
14h (APF)
CC
EC
FSC
B
Lineage
1B1
FSC
FSC-P clone
C
Clone covers 4 follicles before FSC loss
Current FSC not labeled
FSC loss point
Lineage
1B1
FSC-P clone (FSC lost)
C'
FSC
FSC-P lost
FSC
Lineage
1B1
Vas
D
FSC-P lost early
Lineage
1B1
E
Number of Clone
100
80
60
40
20
0
R2b+1
R2b+2
S1
S2-3
S4-5
S6-7
S8+
F
FSC-A
End of clone
Lineage
1B1
Vas
FSC-A clone
G
Lineage
1B1
Vas
G'
Average FSC Clone Coverage: ~50%
H
75%
50%
25%
0%
48.72%
49.68%
By Surface
By Volume
I
R2b+1
R2b+2
S1
Number of Clone
50
40
30
20
10
0
CB Location
FSC-A End
FSC-P Loss
J
Lineage
1B1
Vas
FSC-A
CB clone in R2b
K
Lineage
1B1
FSC-P lost
CB clone passed 2a/2b junction
L
Lineage
1B1
Vas
FSC-P not lost
CB clone before 2a/2b junction

Supporting information for
The Drosophila ovary produces three follicle waves similar to those in mice

Wayne Yunpeng Fu and Allan C Spradling

Corresponding author: Allan C Spradling
Email: spradling@carnegiescience.edu

This PDF file includes:

Supplemental Table S1 to S2
Legends for Supplemental Figures S1 to S4
Legends for Movies S1 to S4

Other supporting materials for this manuscript include the following:

Supplemental Table S3.xlsx

Movies S1 toS4

Supplemental Tables

Table S1

	GSC	R2a	R2b		Stage 1		Stage 2-3		Stage 4-5		Stage 6-7		Stage 8-9		Stage 10A	
	16	16	4-8	16	4-8	16	2-8	16	2-8	16	1-8	16	1-8	16	1-8	16
-2h	18.2%	3.8%	1.7%	9.5%	6.9%	2.6%	10.7%	1.7%	9.8%	1.4%	17.1%	1.2%	17.3%	0.3%	0.6%	0%
2h	18.0%	11.2%	1.0%	16.8%	8.3%	2.6%	16.8%	3.6%	21.5%	2.3%	21.5%	1.0%	26.7%	0.0%	22.1%	0%
6h	17.8%	2.3%	1.6%	11.6%	8.5%	1.6%	11.6%	1.6%	21.7%	0.8%	16.3%	0.8%	37.2%	0%	38.0%	0%
10h	28.9%	6.3%	8.0%	14.7%	16.5%	1.8%	22.8%	2.2%	25.0%	1.8%	39.3%	0%	51.8%	0.4%	10.7%	0%
14h	28.3%	7.9%	10.4%	13.4%	16.5%	2.4%	23.8%	3.0%	34.1%	1.8%	51.8%	0.6%	65.2%	0%	0.6%	0%

Table S1. Germ cell clone quantification. Lineage labeling frequency (number of clones/number of total ovarioles) of germ cell clones at different sizes, stages and HS time points. The first header row indicates the location of recorded germline clones, and the second header row indicates the size of such clones (e.g. 4-8 represents tally of 4-cell and 8-cell germline clones, etc.) For germ cells, only one replicate group is fully quantified due to low level of variation (n=346, 303, 129, 224, 164 ovarioles).

Table S2

	1CC	2CC	1EC	2EC	2+EC	FSC-A	FSC-P (without FSC)	FSC-L (with FSC)
-2h	0.36%	0%	0.65%	0.83%	0.33%	1.05%	1.09%	1.09%
2h	1.36%	0.33%	1.76%	2.34%	0%	2.79%	0.47%	0.56%
6h	1.17%	0.31%	3.43%	1.25%	0.63%	3.03%	0.94%	0.70%
10h	8.48%	3.13%	10.71%	4.91%	7.59%	7.59%	2.68%	4.46%
14h	4.86%	0.58%	8.30%	4.44%	0.72%	6.39%	5.01%	3.27%

Table S2. Somatic cell clone quantification. The percentage are labeling rates of each type of somatic cell clone (number of ovarioles with such clone over the total number of ovarioles). 1CC: clone of 1 cap cell; 2CC: clone of 2 cap cells; 1EC: clone of 1 EC; 2EC: clone of 2 ECs; 2+EC: clone with more than 2 ECs (87% are 4-EC clones); FSC-A: number of short adult FSC clones that correspond to wave 2 follicles (see text); FSC-P (without FSC): number of pupal FSC clones covering wave 1.5 follicles that are missing an active FSC (see text); FSC-P (with FSC): number of long FSC clones that contains an active pupal FSC (see text). n=621, 517, 449, 224, 459 total scored ovarioles.

External Supplemental Tables

Table S3.xlsx. Raw data recording the location and size of each individual observed clone. For interpretation please view the first legends tab inside the excel file.

Supplemental Figures S1 to S4

Figure S1. Additional Information on Experimental Design and PGC biology
A. Schematic showing the detailed recombination process that gives rise to a lineage-labeled cell. **B.** An asymmetry in ovariole formation and PGC distribution exists in early pupal ovary, most prominent at 2h-6h APF and progressively becomes less evident over time. No significant asymmetry is observed by 18h APF. Ovarioles on the top of the image include more germ cells than the ovarioles on the bottom, as indicated by the brackets. PGCs posterior to the ovarioles are also unevenly distributed, more enriched on one side. 3D view shown in Movie S1. **C.** Example ovariole at 30h APF and 40h APF, both lacking the adult 2a/2b junction and R2b cyst morphology. **D-E.** Summary diagrams showing the labeling status of germ cells in wave 1.5 follicles following induction at -2h (F), or 14h (G).

Figure S2. Additional Quantifications of Wave 1 germ cells
A. Quantification of PGCs and cysts in the entire pupal ovary from -2h to 30h APF, showing the extent of PGC symmetric division and the dip caused by wave 1 loss starting at 22h APF. Quantification is based on counting the number of spectrosomes/fusomes, example counting process shown in Movie S2. **B.** Images showing the last rounds of PGC division take place among PGCs that give rise to wave 1.5 follicles at 14h APF. These are the PGCs that become included in the forming ovarioles but are too posterior to become GSCs. No more such divisions are observed at any time point later than 14h APF. **C.** A zoomed-out image of Figure 3N', showing that the single germ cells with vacuole inclusion are indeed GSCs next to the terminal filament, appearing as stacks of DAPI+ flat cells to the left side of the image. **D.** Quantification of wave 1 germ cells (red) and cysts (blue) from 14h to 22h APF. Germ cell count stays the same while cyst number drops from 18h to 22h APF, due to the loss of wave 1 cysts initiating at 22h while the overall number being compensated by continuous cyst division. **E.** Zoomed-in display of the blue "Total Cysts" bars in S2A, detailing the relative proportion of cysts at different sizes in the total population. **F.** A final wave 1.5 follicle now at stage 9 that was lineage labeled at 14h and contains a follicle cell clone which extends to the previous follicle. The border cell cluster at the anterior is mosaic (magnified in the box below) with 3 marked cells, and migrates slower than in adults toward the posterior. Other examples show the large size of the polar cells in these clusters and the presence of 3-4 labeled cells. **G-G'.** More examples showing polar cells migrate posteriorly at different speed than main body follicle cells, while in adults they migrate together. **H-H'''.** Ovarioles of newly eclosed flies showing abnormal cyst size of 8 cells and 32 cells in the last two wave 1.5 follicles, and the disproportionate polyploidization of several nurse cells.

Figure S3. Additional examples of FSC clones
A-A'. Ovarioles with long FSC-P clones that retained an active pupal FSC. **B-C.** Examples of FSC-A clones. C' is the magnified germarium region of the ovariole in C. **D-D'.** Ovarioles with long FSC-P clones that do not contain an active pupal FSC, replaced by an unlabeled FSC. **E-E'.** Short FSC-P clones on the older wave 1.5 follicles that had an early FSC loss. **F-F'.** The shortest FSC-P clones that only cover the anterior of oldest wave 1.5 follicle, complementing the basal stalk follicle cell clone shown in G-G'. **G-G'.** Small patches of follicle cell clone that only cover

the most mature wave 1.5 follicles, most likely originating from the basal stalk cells as previously reported (Reilein et al. 2021).

Figure S4. Lineage labeled escort cell (EC) clones.
A. A germarium stained to mark the ECs using the enhancer trap line PZ1444. Two GSCs (unlabeled) are seen at the front associated with cap cells (arrowhead). In addition, 8 specific ECs are labeled and indicated with arrowheads and assigned corresponding names. B-L show germaria following clonal marking to identify EC-specific clones. **B-B''.** Example germaria each with one labeled EC1 (arrows). **C-C'.** Germaria with single EC2 clone. **D.** Germarium with an EC3 clone. **E-E'.** Germaria with single EC5 clone. **F-F'.** Examples of EC6 clone, immediately next to FSCs. **G.** An EC6 clone in the middle of the germarium at 2a/2b junction. **H.** Labeling frequency of EC clones based on the number of ECs each clone contains. **I.** Frequency of ovarioles with clones of ECs by type (EC1-6). **J.** Two adjacent labeled ECs, E5 and E4 are located directly adjacent to an unlabeled FSC. **J'.** An ovariole containing 4 ECs that are close to the 2a/2b junction. **K-K''.** Examples of cap cell clones. K' contains 2 labeled cap cells. **L.** An ovariole containing both a CB clone and a FSC-P clone that has lost its active pupal FSC, showing FSC-P loss happened slightly after the CB clone passed by 2a/2b junction.

Legends for Movies S1 to S2

Movie S1: Rotation of a 6h APF ovary showing the asymmetry of PGC distribution along a dorsal-ventral axis.

Movie S2: Example process of PGC counting in the pupal ovary. Spectrosomes/fusomes shown as magenta dots stained by Hts/1B1 are circled, as they are counted in Imaris using the Spot function.

Movie S3-S4: Examples showing how the quantification of follicle cell coverage in Figure 5K-L was done in Imaris in 3D reconstruction. Movie S3 shows an FSC-L clone and Movie S4 shows an FSC-M clone.

Figure S1

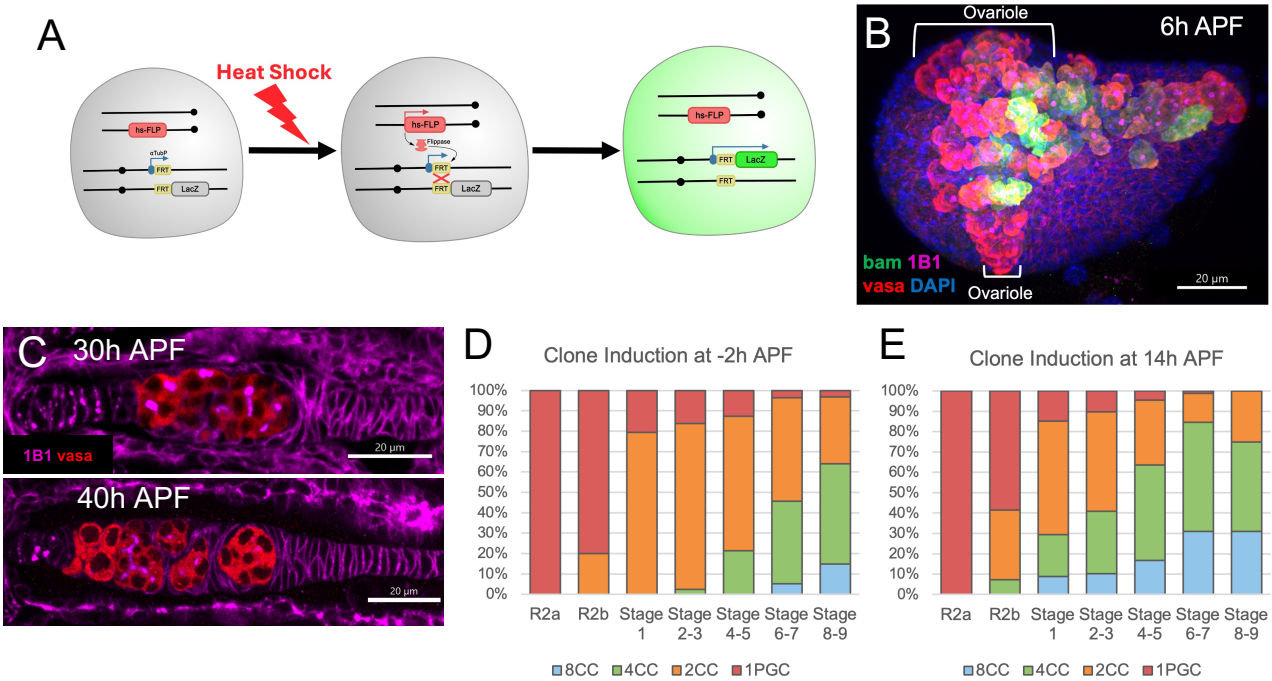
A
Heat Shock
hs-FLP
αTubP
FRT
LacZ
Flippase
B
Ovariole
6h APF
bam 1B1
vasa DAPI
20 µm
C
30h APF
1B1 vasa
40h APF
D
Clone Induction at -2h APF
E
Clone Induction at 14h APF
100%
90%
80%
70%
60%
50%
40%
30%
20%
10%
0%
R2a
R2b
Stage 1
Stage 2-3
Stage 4-5
Stage 6-7
Stage 8-9
8CC
4CC
2CC
1PGC

Figure S2

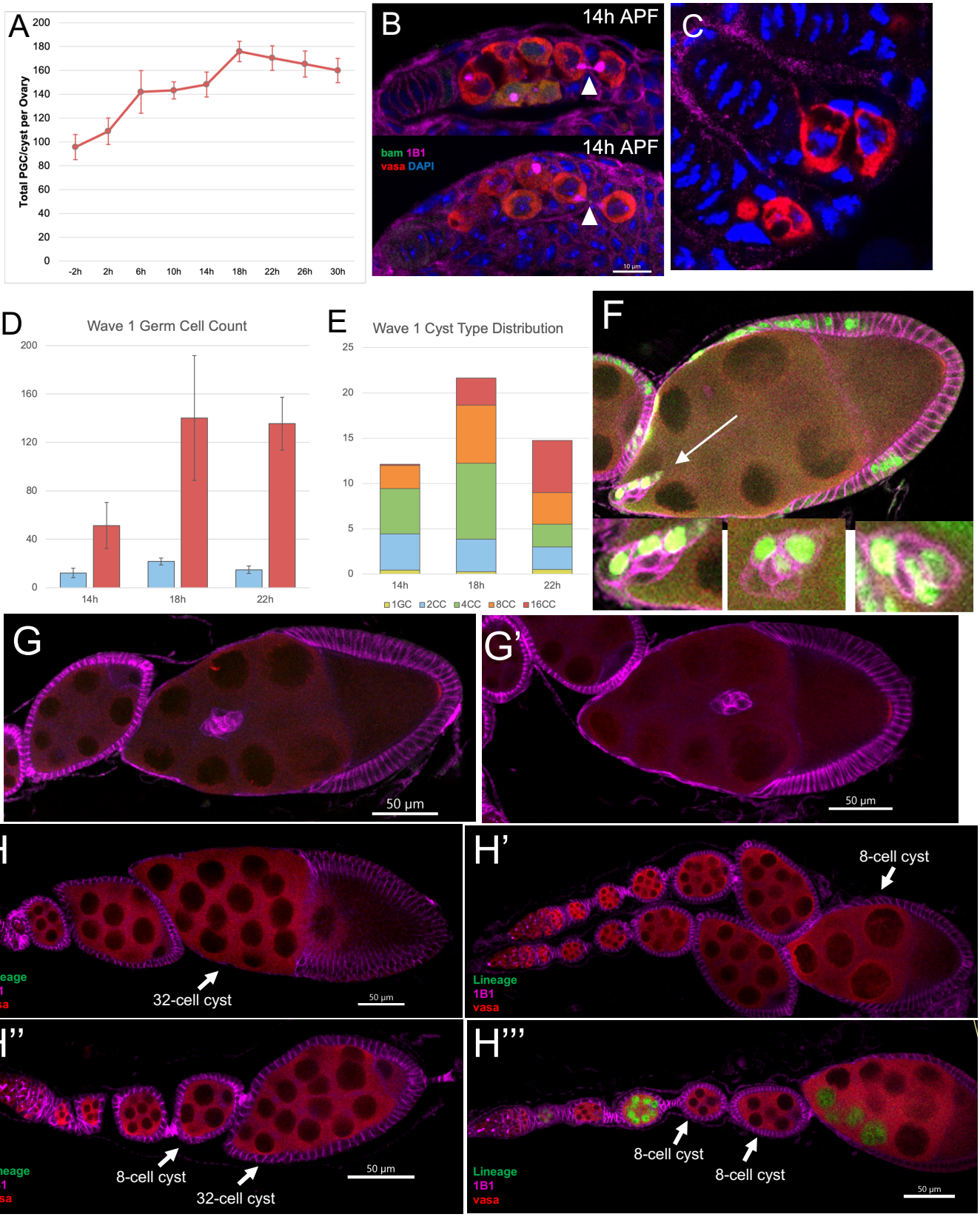
A
Total PGC/cyst per Ovary
200
180
160
140
120
100
80
60
40
20
0
-2h
2h
6h
10h
14h
18h
22h
26h
30h
B
14h APF
bam 1B1
vasa DAPI
14h APF
10 µm
C
D
Wave 1 Germ Cell Count
200
160
120
80
40
0
14h
18h
22h
E
Wave 1 Cyst Type Distribution
25
20
15
10
5
0
14h
18h
22h
1GC
2CC
4CC
8CC
16CC
F
G
50 µm
G'
50 µm
H
Lineage
1B1
vasa
32-cell cyst
50 µm
H'
8-cell cyst
Lineage
1B1
vasa
H''
Lineage
1B1
vasa
8-cell cyst
32-cell cyst
50 µm
H'''
8-cell cyst
8-cell cyst
Lineage
1B1
vasa
50 µm

Figure S3

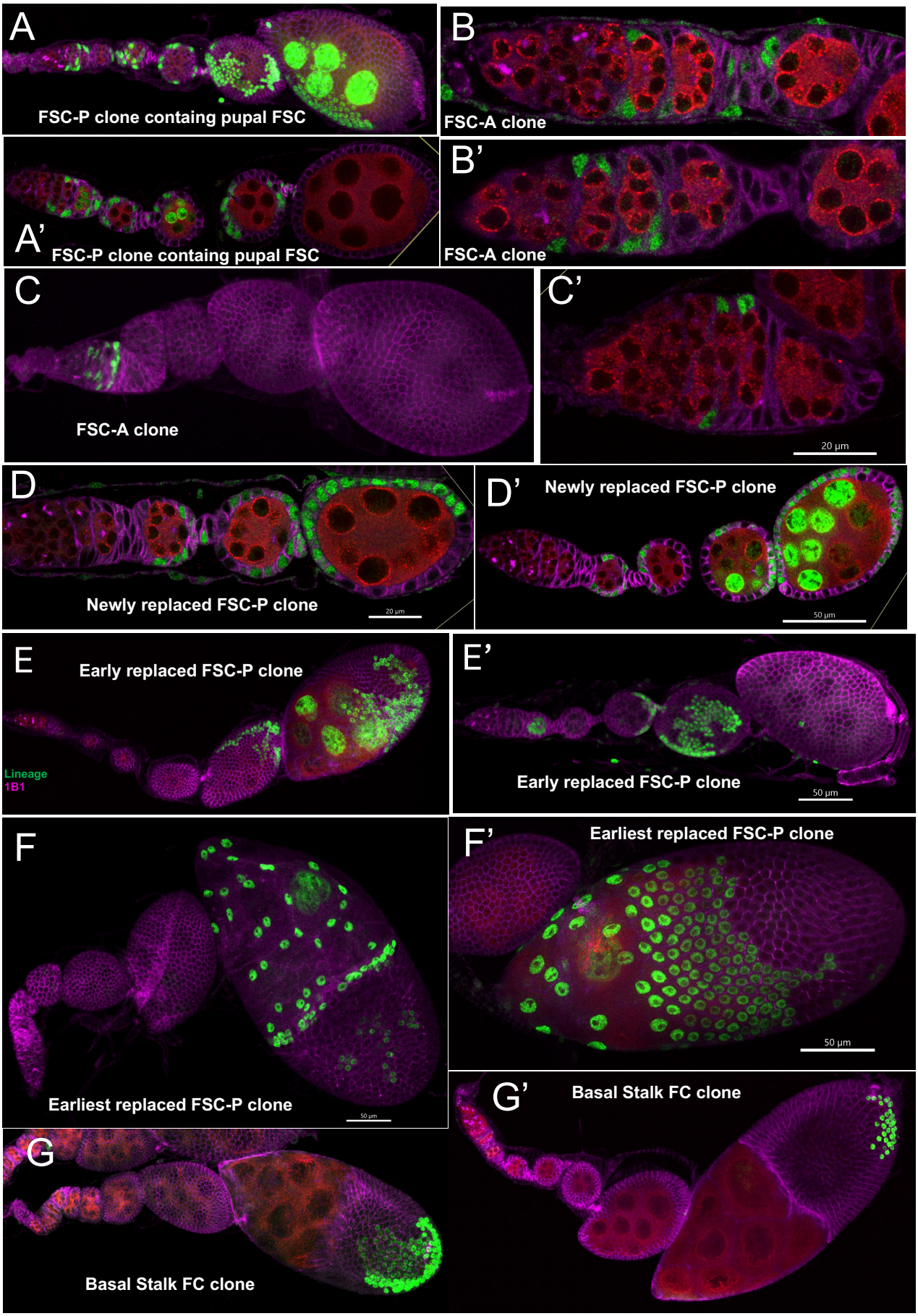
A
FSC-P clone containg pupal FSC
B
FSC-A clone
A'
FSC-P clone containg pupal FSC
B'
FSC-A clone
C
FSC-A clone
C'
20 µm
D
Newly replaced FSC-P clone
20 µm
D'
Newly replaced FSC-P clone
50 µm
E
Early replaced FSC-P clone
Lineage
1B1
E'
Early replaced FSC-P clone
50 µm
F
Earliest replaced FSC-P clone
50 µm
F'
Earliest replaced FSC-P clone
50 µm
G
Basal Stalk FC clone
G'
Basal Stalk FC clone

Figure S4

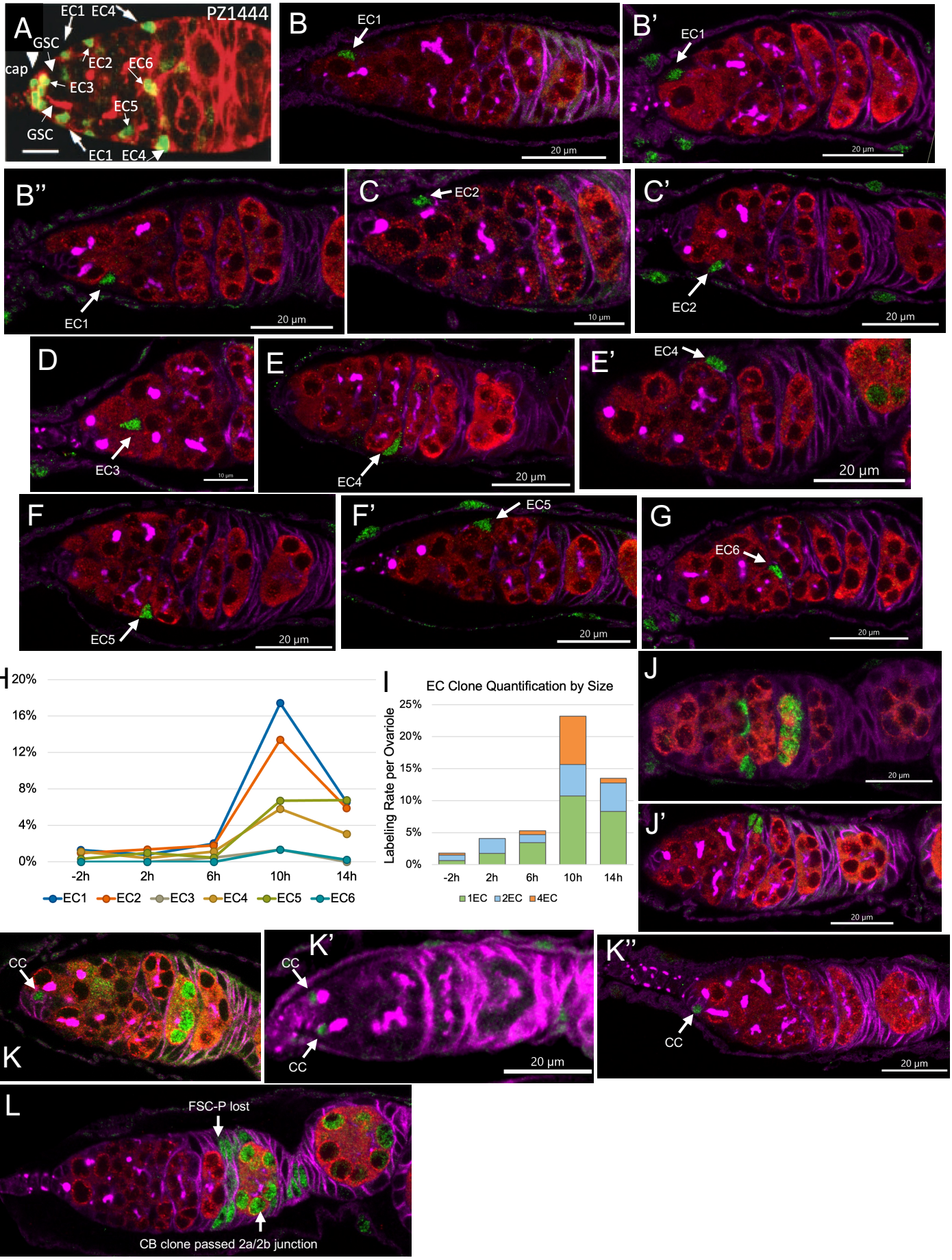
A
PZ1444
EC1 EC4
GSC
cap
EC2
EC6
EC3
EC5
GSC
EC1 EC4
B
EC1
20 µm
B'
EC1
20 µm
B''
EC1
20 µm
C
EC2
10 µm
C'
EC2
20 µm
D
EC3
10 µm
E
EC4
20 µm
E'
EC4
20 µm
F
EC5
20 µm
F'
EC5
20 µm
G
EC6
20 µm
H
20%
16%
12%
8%
4%
0%
-2h
2h
6h
10h
14h
EC1 EC2 EC3 EC4 EC5 EC6
I
EC Clone Quantification by Size
Labeling Rate per Ovariole
25%
20%
15%
10%
5%
0%
-2h
2h
6h
10h
14h
1EC 2EC 4EC
J
20 µm
J'
20 µm
K
CC
K'
CC
CC
20 µm
K''
CC
20 µm
L
FSC-P lost
CB clone passed 2a/2b junction